Biomaterials 33 (2012) 6660–6671

Contents lists available at SciVerse ScienceDirect

Biomaterials

journal homepage: www.elsevier.com/locate/biomaterials

The effect of intraluminal contact mediated guidance signals on axonal mismatch during peripheral nerve repair

William T. Daly [a], Li Yao [a,b], Mohammad T. Abu-rub [a], Claire O'Connell [c], Dimitrios I. Zeugolis [a], Anthony J. Windebank [d], Abhay S. Pandit [a,*]

[a] Network of Excellence for Functional Biomaterials (NFB), National University of Ireland, Galway, Ireland
[b] Wichita State University, 1845 Fairmount, Wichita, KS 67260, USA
[c] National Centre for Laser Applications (NCLA), National University of Ireland, Galway, Ireland
[d] Mayo Clinic, Rochester, MA, USA

ARTICLE INFO

Article history:
Received 23 April 2012
Accepted 2 June 2012
Available online 25 June 2012

Keywords:
Nerve guidance conduit
In vivo
Biomaterials
Peripheral nerve
Repair
Nerve guide

ABSTRACT

The current microsurgical gold standard for repairing long gap nerve injuries is the autograft. Autograft provides a protective environment for repair and a natural internal architecture, which is essential for regeneration. Current clinically approved hollow nerve guidance conduits allow provision of this protective environment; however they fail to provide an essential internal architecture to the regenerating nerve. In the present study both structured and unstructured intraluminal collagen fibres are investigated to assess their ability to enhance conduit mediated nerve repair. This study presents a direct comparison of both structured and unstructured fibres *in vivo*. The addition of intraluminal guidance structures was shown to significantly decrease axonal dispersion within the conduit and reduced axonal mismatch of distal nerve targets ($p < 0.05$). The intraluminal fibres were shown to be successfully incorporated into the host regenerative process, acting as a platform for Schwann cell migration and axonal regeneration. Ultimately the fibres were able to provide a platform for nerve regeneration in a long term regeneration study (16 weeks) and facilitated increased guidance of regenerating axons towards their distal nerve targets.

1. Introduction

Treatment of peripheral nerve injuries is currently limited to a small number of microsurgical treatment methods. These treatments are ineffective as these interventions often lead to painful neuropathies as a result of loss in motor control and sensory perception [1,2]. Over relatively short nerve gaps, spontaneous natural regeneration may occur. However, over larger gaps, microsurgical repair is essential for nerve regeneration [3–5]. The primary methods of repair include direct/primary repair, transplantation of autografts or allografts, and the use of hollow nerve guidance conduits [6]. Direct repair is limited to treating short nerve defects (<5 mm in length) and requires tension-free suturing of the damaged nerves [7,8].

Beyond this relatively short gap, autografting is the current gold standard for repair. Despite providing a number of advantages for repair, success in the clinic has been limited. This is partly due to a number of the intrinsic limitations of the gold standard, particularly nerve and axonal size mismatches between the donor nerve and the targeted injured nerve [6,9]. In addition there is a requirement for a second surgical site i.e. donor site that has a limited supply of nerve. Donor site complications often lead to morbidity and pain. Despite these limitations, autograft healing is characterised by some intrinsic ideal components for peripheral nerve repair. Autograft provides a natural architecture for guided nerve regeneration, as well as being readily incorporated into the regenerative process; due to the graft being derived from the host's own tissue. The intrinsic network of extracellular matrix proteins and cell adhesion molecules provides regenerating axons, and migrating and proliferating Schwann cells (from the proximal and distal nerve stumps) with appropriate topographical and biological guidance cues to achieve functional nerve regeneration [10]. To recreate this natural internal architecture for repair an extracellular matrix derived platform (i.e. one made from collagen, fibronectin or laminin) often proves useful for repair [11–13].

In efforts to reconstruct this architecture this study proposes the use of a natural extracellular matrix protein (i.e. collagen) based construct which displays topographical features and structural characteristics which are beneficial for repair. This investigation

* Corresponding author. Tel.: +353 91492758.
E-mail address: abhay.pandit@nuigalway.ie (A.S. Pandit).

0142-9612/$ – see front matter © 2012 Elsevier Ltd. All rights reserved.
http://dx.doi.org/10.1016/j.biomaterials.2012.06.002

incorporates such a system in the form of intraluminal collagen fibres into the lumen of a hollow nerve guidance conduit. Hollow nerve guidance conduits are the commercial alternatives to grafting and have a number of advantages for repair. These advantages include limiting myofibroblast infiltration, a reduction in scar and neuroma formation, and no associated donor pain [14]. However, hollow conduits provide only limited structural support (in the form of a fibrin cable) and guidance to regenerating axons and as a result functional recovery remains poor [6,8,15]. To overcome the limitations of the use of hollow conduits, intraluminal guidance structures (e.g. fibres, films, gels) are used to supplement/replace the fibrin cable and/or to recreate the natural topographical features of autograft [12,16–20]. This study uses intraluminal biologically derived collagen fibres for such a purpose. Ultimately, the addition of these extracellular matrix (ECM) derived components aims to recreate the hierarchical organisation and biological function of the native extracellular matrix. This investigation thoroughly analyses the incorporation of these components into the host regenerative process and assesses their feasibility for improving or enhancing conduit mediated nerve repair. In particular this study investigates the influence of intraluminal fibres on the levels of axonal dispersion within the biomaterial conduit.

In addition this study incorporates a number of longitudinal grooves on the surface of the collagen fibres for additional topographical guidance (Fig. 1). The use of topographical guidance cues has shown to have beneficial effects for nerve repair. Topographical cues have been shown to introduce complex signalling responses within the growth cone of a regenerating and have resulted in profound changes in the neuronal response to injury [21]. Structural cues have been incorporated on a number of substrates *in vitro* resulting in a significant increase in aligned neurite outgrowth [21–23]. This increase in neurite alignment and growth is accompanied by a significant reduction in the number of neurites and neurite branching. Mahoney et al. demonstrated increased alignment and growth of PC12 cells on micro-structured polyimide for features in the range of 20–30 μm versus features which had a width of 40–60 μm [24]. Preliminary work by our own group demonstrated increased aligned growth of PC12 neurites on micro-structured PLGA film with features ranging from 5 to 10 μm in width [25]. Based on these results, topographical guidance features have been combined with the aforementioned intraluminal guidance structures in the form of structured collagen fibres to assess their combined ability to enhance peripheral nerve repair.

2. Materials and methods

2.1. Extrusion and crosslinking of collagen fibres

The extrusion procedure and crosslinking were carried out in the same manner as reported by Zeugolis et al. [26,27]. A 5 ml syringe (BD Scientific, UK) containing 5 mg/ml bovine type I atellocollagen was extruded at a rate of 0.3 ml/min by a syringe pump (KD-Scientific 200, KD-Scientific Inc., Massachusetts, USA) through 0.03 mm inner diameter silicone tubing (Polymer Technologies Ltd, Warwickshire, UK) into a fibre formation buffer (118 mM phosphate buffer and 20% of polyethylene glycol, M_w 8000, pH 7.50 and 37 °C). Fibres were allowed to remain in the fibre formation buffer for 5 min and transferred into a fibre incubation buffer (6.0 mM phosphate buffer and 75 mM sodium chloride; pH 7.10 and 37 °C) for a further 5 min.

The extruded collagen fibres were subsequently cross-linked with N-(3-dimethylaminopropyl)-N-ethylcarbodiimide (EDC) and N-hydroxysuccinmide (NHS), at a ratio of 30 mM:10 mM respectively, in 50 mM MES buffer (pH 5.5), for 24 h. After this period, the fibres were rinsed three times with sterile distilled water and allowed to air-dry, under the tension of their own weight. Similarly, for non-cross-linked collagen fibres, fibres were briefly dipped in distilled water for

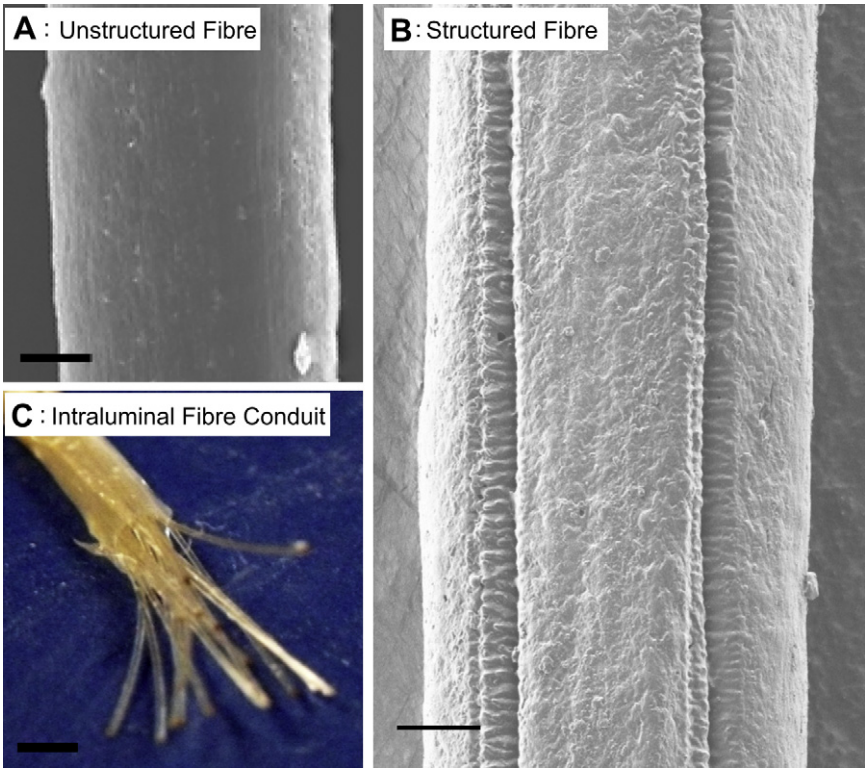

Fig. 1. Images of unstructured and structured collagen fibres and their incorporation into a hollow collagen nerve guidance conduit. (A) SEM image of an unstructured collagen fibre with a diameter of approximately 50 μm. Scale bar, 10 μm. (B) SEM image of structured collagen fibre with four channels on the surface of the fibres (channel diameter 10 μm). Scale bar, 10 μm. (C) Photo of a conduit with 18 structured collagen fibres inserted into the lumen of a hollow collagen nerve guidance conduit. Fibres are shown to be protruding from the lumen of the conduit. For implantation, fibres are trimmed to a length of 10 mm and inserted into a 12 mm long hollow nerve guidance conduit. This allows the proximal and distal nerves to be implanted into the conduit without inducing axial compression on the intraluminal fibres. Scale bar, 1.5 mm.

Table 1
List of the treatment groups and number of animals used for the current *in vivo* study and the experimental procedures (nerve morphometry and retrograde tracing) carried out on each respective group.

Treatment group	Nerve morphometry (No. of animals)	Retrograde tracing (No. of animals)	Nerve gap (cm)
Autograft	8	6	1
Hollow collagen conduit	8	6	1
Unstructured fibres	8	6	1
Structured fibres	8	6	1

approximately 1 min and then allowed to dry under the tension of their own weight for 24 h. The diameter of the collagen fibres were measured using an IX81 inverted microscope (Mason Technology, Dublin, Ireland). The degree of crosslinking was confirmed via the ninhydrin assay.

2.2. Fabrication of structured collagen fibres

Microgrooves were produced on the surface of the collagen fibres using an excimer laser (ATL Atlex®, Wermelskirchen, Germany) in conjunction with a machining centre (Optec MicroMaster®, Frameries, Belgium). Argon fluoride gas (Spectra Gases, UK), with a 3–7 ns pulse duration, was chosen as the active laser medium for the laser. Argon fluoride gas allows operation of the laser at a wavelength of 193 nm, which results in the clean ablation of a large range of materials in particular biological substrates. This allows structuring of the collagen fibres without damage to the underlying substrate [28]. A pulse repetition frequency of 100 Hz with a constant speed of 500 μm/s was selected to give the optimal compromise of process speed and feature accuracy. The microgrooves were generated using a standard mask projection machining approach. For each parameter, a different dimensioned mask was used with a varied demagnification, to produce topographical features of defined width and depth (Table 2).

A rotary stage was used in conjunction with the aforementioned excimer laser system to create micro-structured fibres with multiple grooves orientated longitudinally across its surface (Fig. 1). Structuring of the surface was confirmed using a scanning white light interferometric surface profiler (NewView 100, Zygo, Middlefield, CT, USA) and Scanning Electron Microscopy (SEM) (Phenom™ Desktop Scanning Electron Microscopy FEI®, Eindhoven, The Netherlands).

2.3. Characterisation of collagen fibres

Characterisation of the micro-structured fibres was carried out in the Advance Microscope Facility (Centre of Research on Adaptive Nanostructures and Nanodevices, Trinity College Dublin) on a Carl Zeiss Auriga® focused ion beam (FIB) system. Depth measurements and groove widths were quantified using this SEM – FIB system. Briefly, samples were sputter-coated (Cressington 208 HR sputter coating system) with a protective 10 nm palladium over layer and grounded with silver paint. Samples were mounted in the FIB mounting chamber and a SEM image of each section was taken. The sample stage was tilted from 0° to 54° to determine a suitable site for cross-sectioning. Upon location of a suitable region of interest, FIB cross-sections were taken at high beam currents, and subsequent polishing of the surface performed at lower beam currents and SEM images taken of the sectioned region. This technique allowed for an accurate analysis of groove width and depth measurements from the cross section (Table 2).

2.4. Preparation of intraluminal conduits and experimental groups for in vivo implantation

Intraluminal conduits were constructed by enclosing 18 collagen fibres within a hollow collagen conduit. These conduits were then filled with structured and non-structured collagen fibres respectively. Structured fibres of approximately 50 μm diameter and 4 longitudinal channels (10 μm widths and a high depth) were used for all *in vivo* experimentation. Samples were sterilised by a 2 h incubation period in 70% ethanol, rinsed in sterile 0.1 M phosphate buffer and stored until use. 56 adult female Lewis rats weighing between were between 220 and 250 g were randomly assigned to one of four experimental groups (Table 1). Two experimental procedures were carried out for each experimental group: both nerve morphometry ($n = 8$) and simultaneous retrograde tracing ($n = 6$) analyses. All experimental procedures were carried out in accordance to National and Institutional guidelines set out by the Cruelty to Animals Act 1876 as amended by the European Communities (Amendment of Cruelty to Animals Act, 1876) Regulations 2002 & 2005.

Table 2
Parameters for excimer laser structuring of the extruded collagen fibres and resulting diameters and depths of the micro-structured fibres.

Targeted groove diameter (μm)	Actual mean diameter (±SD) (μm)	Mean depth (±SD) (μm)	Fluence used (mJ/cm^2)	Speed (μm/s)	Rep. rate (Hz)
2.5	3.45 (±0.32)	3.81 (±0.52)	176	250	100
5 (low depth)	5.09 (±0.50)	3.17 (±0.94)	86	500	100
5 (high depth)	4.80 (±0.44)	5.92 (±0.82)	120	500	100
10 (low depth)	9.65 (±0.55)	6.77 (±0.34)	130	500	100
10 (high depth)	11.08 (±1.11)	8.55 (±0.72)	233	500	100

2.5. Surgical procedure

Rates were anesthetised by intraperitoneal injection under aseptic conditions. The left sciatic nerve was exposed and isolated at the mid-thigh level using a dorsal glutaeal muscle splitting approach. The nerve was resected 5 mm proximally from the distal bifurication of the tibial and peroneal branches and a 5 mm nerve segment was removed, resulting in the creation a 10 mm nerve gap. The proximal and distal ends of the transected nerve were inserted 1 mm into 12 mm long collagen tubes (with/without intraluminal fillers) and secured to the epineurium using 10-0 monofilament nylon sutures (Ethicon, Location). The wound was finally closed in layers and the animals received buprenorphine hydrochloride for the treatment of pain. Animals were continuously monitored for signs of distress or pain. For autograft repair the nerve were similarly transected at two different sites, approximately 1 cm apart, rotated 180° and re-attached to the transected nerve stumps, using 10-0 nylon sutures (Johnson & Johnson, Dublin, Ireland).

2.6. Nerve histology

Sixteen weeks post-implantation, the sciatic nerve was re-exposed under anaesthesia. The exposed sciatic nerve was fixed *in situ* using Trump's fixative solution (4% formaldehyde, 1% glutaraldehyde in 0.1 M phosphate buffer saline solution) for 30 min [29]. The fixative solution was removed from the injury site, and the sciatic nerve was resected and divided into three 1 mm sections: 1 mm proximal to graft, midgraft and 1 mm distal to the graft. The sections were placed in the Trump's fixative solution and stored for sectioning. Sections from the midsection of the nerve were post-fixed in 1% osmium tetroxide solution and passed through of series of graded alcohol solutions for serial dehydration of the samples. Sections were embedded in spur resin (EMS, Fort Washington, USA) and 1 μm semi-thin sections were cut using a glass knife on a Leica UltraCut E® Microtome (Rankin Biomedical Corp., Michigan, USA), stained with 1% toluidine blue and mounted for light microscopy and subsequent electron microscopy.

2.7. Morphology and stereology

The midsection of the resected nerve was quantified for axonal area, number of axons, axonal density, diameter of axons, and diameter of myelinated fibres, myelin thickness, axonal size distribution and g-ratio (Fig. 9). G-ratio was taken as the ratio of inner axonal diameter to the total axonal diameter and was used as a functional index of myelination. The ideal g-ratio was taken to be approximately between 0.6 and 0.7 [30]. All parameters were quantified using an upright florescent microscope (BX51 Upright Fluorescent Microscope®; Olympus Inc.) and analysed using ImageJ image analysis software (NIH, Bethesda, USA). The nerve area was quantified via tracing of the circumference of the regenerated tissue at 100× magnification. Axonal counts were quantified stereologically at 1000× magnification using the area fraction method [31]. This method allows all axons to be equally sampled from the total nerve area. A 1600 μm^2 area was taken and counted using an unbiased counting frame and repeated in a systematic and random manner (Fig. 8). The number of axons per unit area was calculated and extrapolated to the total nerve area to give total nerve counts for the section. Similarly, the fibre and axon size distribution, average axon and myelinated fibre diameters, and myelin thickness were similarly counted. A minimum of 50 axonal profiles per sample were evaluated using this method.

2.8. Simultaneous retrograde tracing

At week 16, the sciatic nerve was re-exposed, at the location where the tibial and peroneal nerves branch off the sciatic nerve (Fig. 3). Distal from this branching point, the tibial and peroneal nerves were transected. The proximal end of the cut peroneal nerve was initially placed in a 5% diamidino yellow solution (Sigma Aldrich, Co. Wicklow, Ireland) for 30 min. Subsequently the cut end of the tibial nerve was exposed to 5% fast blue solution (Sigma Aldrich, Co. Wicklow, Ireland) for further 30 min. After exposure, the cut ends of the nerves were washed with 0.9% saline solution and were sutured back into the surrounding tissue to prevent leakage of the dye. Seven days after tracer application, the animals were transcardially perfused with 4% paraformaldehyde and 10% sucrose in phosphate buffered solution (PBS) and the spinal cord segments L1 to L6 were removed and post-fixed overnight. Sagittal longitudinal sections were embedded in Cyro-gel™ (Instrumedics Ltd, St Louis, MO) and 30 μm thick sections were cut on a cryostat (Microm HM505E Cryostat®, Walldorf) at −20 °C. Sections were immediately evaluated under an

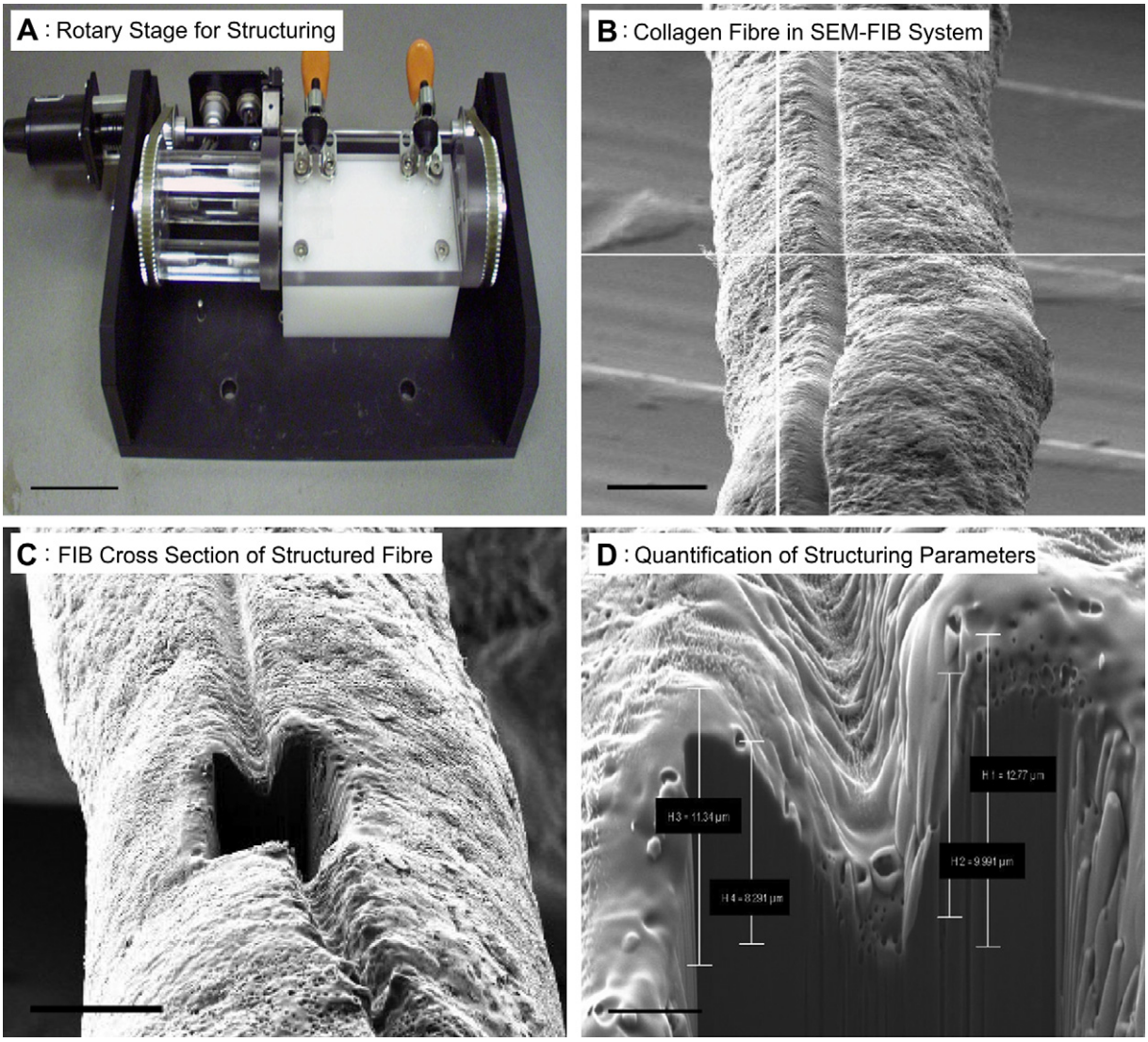

Fig. 2. Excimer laser rotary stage setup for structuring of the fibres and scanning electron microscope images of the SEM-FIB process. (A) Photograph of the fabricated rotary stage used to hold the collagen fibres in place during structuring. Stage worked readily with the excimer laser systems own software package to allow precise control of the rotation of the fibres and alignment of the excimer laser. Scale bar, 5 cm. (B–D) SEM images of the sequence of events in the SEM-FIB process. A suitable region of interest was identified as in (B) and the sample was rotated to 54° for structuring. High focus ion beam currents were used to generate the cross section and subsequent polishing of the cross section was performed at lower beam currents. The resulting cross section can be seen in (C). Quantification of the cross section parameters was performed at higher magnification as in (D). Scale bars, 50 μm (B and C), 1 μm (D).

upright fluorescent microscope (BX51 Upright Fluorescent Microscope®; Olympus Inc.). Neuronal profiles with blue cytoplasm and a dark nucleus were counted as FB-labelled neurons, profiles with a yellow nucleus and dark cytoplasm as DY-labelled neurons, and profiles with a yellow nucleus and blue cytoplasm as FB/DY-double-labelled neurons. All neurons in each section were counted.

2.9. Statistical analysis

All graphical data is presented as mean ± standard error of the mean (S.E.M.). Graphpad™ v5.1 (Graphpad Software, California, USA) statistical analysis software was used for all statistical analysis. Statistical analysis included a one way analysis of variance (ANOVA) followed by a Tukey *post hoc* test for multiple comparisons. A p value of 0.05 was deemed statistically significant.

3. Results

3.1. Fabrication and characterisation of intraluminal collagen fibres

Intraluminal collagen fibres were fabricated using a fibre extrusion process (Fig. 1). These fibres were approximately 50 μm in diameter and were cross-linked using EDC:NHS at a ratio of 30 mM:10 mM to increase their strength, lower their degradation rate and to maintain their structural integrity *in vivo*. The degree of crosslinking was confirmed using a ninhydrin assay. This assay showed a significant reduction in the number of free amines in the cross-linked group versus the control non-cross-linked collagen fibres group ($p < 0.05$).

The cross-linked fibres were subsequently structured using an excimer laser system that was linked to a machining centre that produced the defined topographical features (Figs. 1 and 2). For depth measurements SEM combined with FIB cross-sectioning was used (Fig. 2). This analysis provided accurate measurements of the surface architecture of the collagen fibres after ablation of the surface (Table 2). Using the excimer laser system, a range of fibre diameters and depths were produced. These results assessed the ability to produce reproducible topographical features of controlled depth and width.

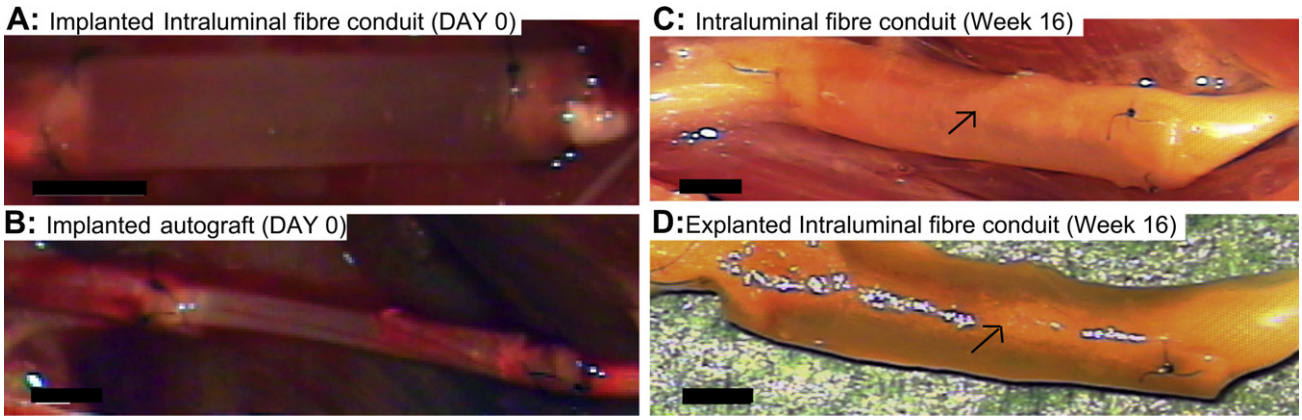

Fig. 3. Microscopic images of surgical implantation of conduit groups and autograft at Day 0 (A and B) and images of explanted NGCs after 16 weeks *in vivo* (C and D). (A) Representative image of conduit groups implantation. (B) An implanted autograft is secured in place with two 10-0 nylon sutures on Day 0. (C) An explanted nerve guidance conduit showing a regenerated tissue cable running proximal to distal 16 weeks after implantation. (D) *In vivo* image of structured fibre conduit showing a defined regenerated tissue cable after 16 weeks *in vivo*.

3.2. Surgical outcome of implanted intraluminal guidance conduits

Conduits were implanted in all animals; with only 10% of animals displaying minimum signs of irritation. 16 weeks post-implantation, all animals survived the entire period of implantation. At the defined endpoint, all conduits showed no signs of collapse (with minimum signs of premature degradation) and a tissue cable was seen to be present throughout the conduit for all

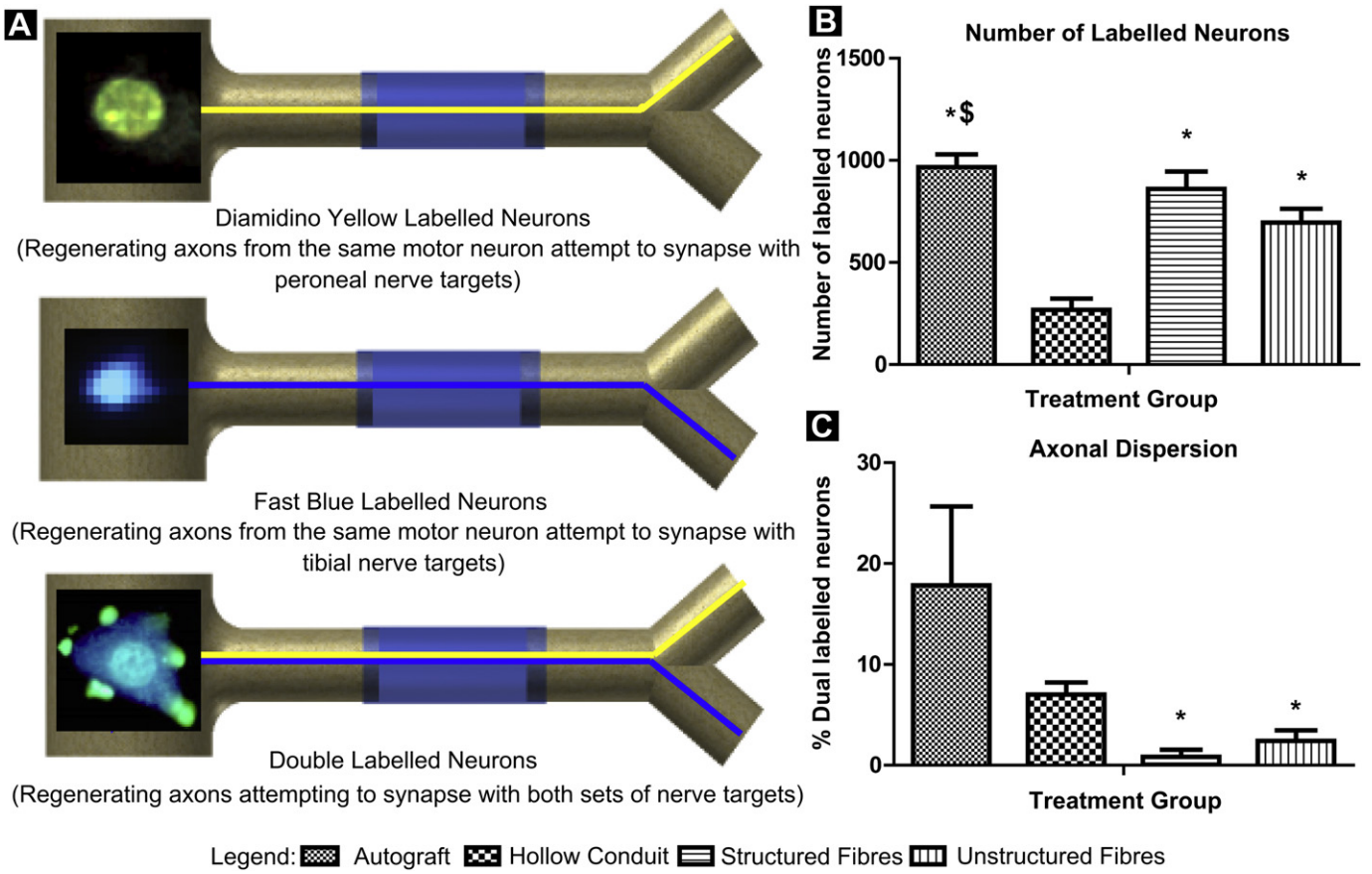

Fig. 4. Retrograde tracing results. (A) Schematic drawing of the concept of simultaneous retrograde tracing. A diamidino yellow dye is applied to the peroneal branch of the sciatic nerve. The dye is applied to the nerve for a period of 30 min to allow adequate absorption of the dye. The dye is subsequently transported retrograde to the spinal column over a period of 1 week. The absorption and transport of the dye will label the nuclei of the associated neurons yellow. This confirms regeneration of axons down the peroneal branch of the nerve and that the same motor neurons are attempting to reinnervate peroneal nerve targets. The fast blue dye is simultaneously applied at the same initial time period to the tibial nerve and allowed to be transported retrograde in the same manner as the aforementioned dye. Fast blue dye absorption will label the cytoplasm of the neurons with a blue colour. This confirms regeneration down the tibial nerve branch and that the same neurons are correctly attempting to reinnervate tibial nerve targets. Finally if both dyes are present in the same neuron (yellow nucleus, blue cytoplasm) then it can be concluded that one neuron is incorrectly attempting to synapse with both peroneal and tibial nerve targets. (For interpretation of the references to colour in this figure legend, the reader is referred to the web version of this article.)

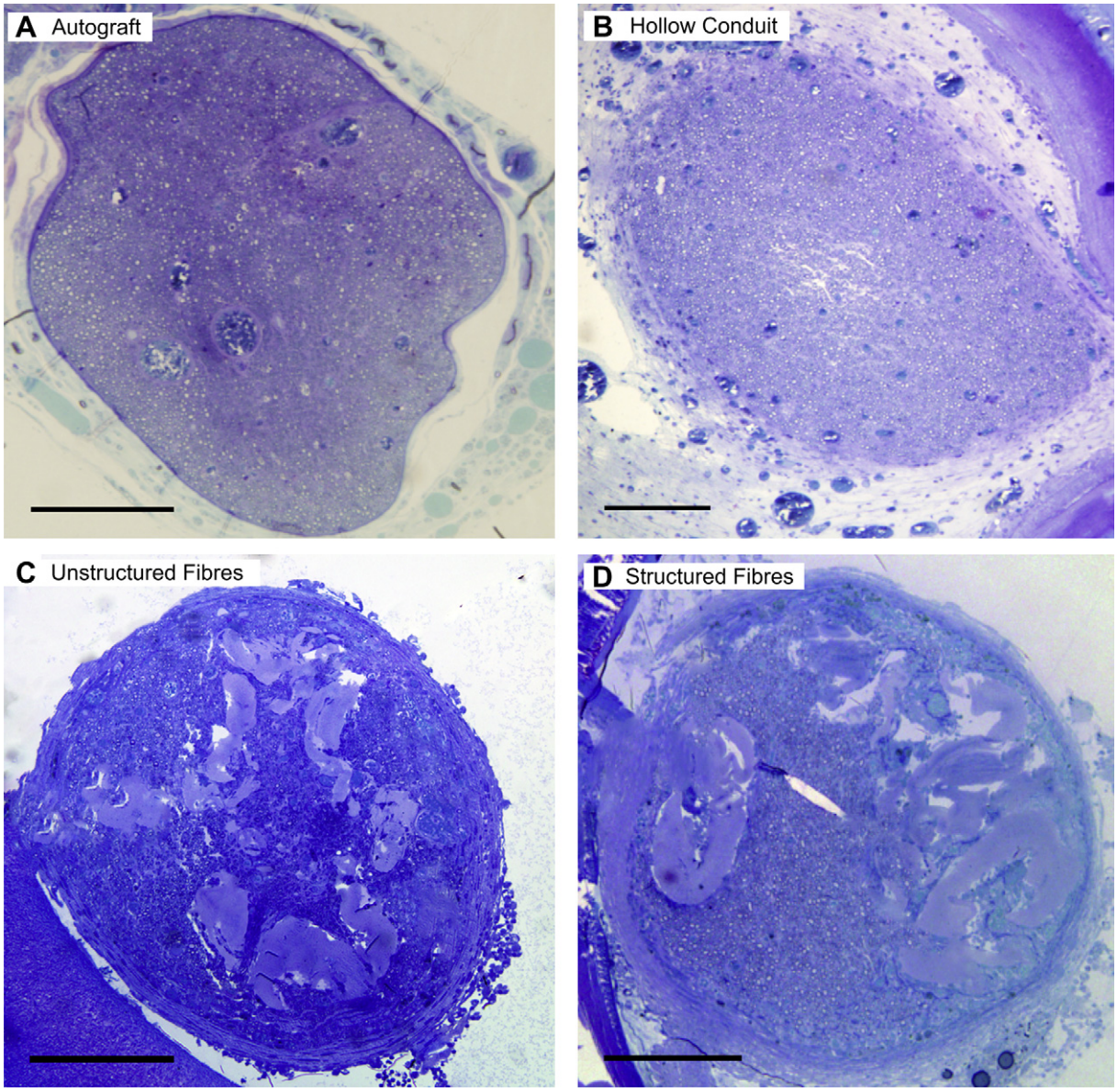

Fig. 5. Histological overview of the regenerated nerve cables seen present at the midgraft level of each of the experimental groups as follows: (A) autograft (B) hollow conduit (C) structured fibre conduit and (D) unstructured fibre conduit. In both of the collagen fibre groups, fibres can be seen to have successfully been incorporated into the regenerative process with little to no apparent foreign body response. Fibres appear to have been reduced in area from the original circumferential area it is likely that the fibres at this stage have begun to partially degrade. All scale bars: 100 μm.

implanted groups (Fig. 2). One instance of neuroma was noted for the autograft group and was excluded from further analysis.

3.3. Simultaneous retrograde tracing – innervation of distal targets

One week after exposure to the retrograde tracing dyes, the spinal column was removed and the L1-L6 segments of the spinal cord were isolated and sectioned for assessment. After sectioning, the number of fast blue (FB), diamidino yellow (DY) and double-labelled (DL) motor neurons were counted to assess the number of axons approaching their distal targets and the degree of misdirection of regenerated nerves. The total number of neurons was calculated by summing all the labelled profiles (i.e. FB + DY + DL) and comparing between groups. Retrograde tracing results showed a significantly higher total number of labelled neurons in both the structured fibres and unstructured groups versus the control hollow conduit ($p < 0.05$). This suggests that statistically more regenerating axons are growing through their respective branches towards their distal targets versus control hollow conduits, at the point of the retrograde dye application (Fig. 3). The regenerating axons may not however have reached their distal targets. The total number of neurons in the structured fibres group was not statistically different to that of the autograft group.

The number of misdirected axons was calculated by dividing the number of dual labelled motor neurons by the total number of motor neurons. This allowed calculation of the percentage of misdirected axons. A significant reduction in the number of misdirected axons was seen in both the structured and unstructured fibre groups (0.84% ± 1.19% and 2.42% ± 2.33%) respectively versus the autograft group (17.83% ± 13.57%) ($p < 0.05$).

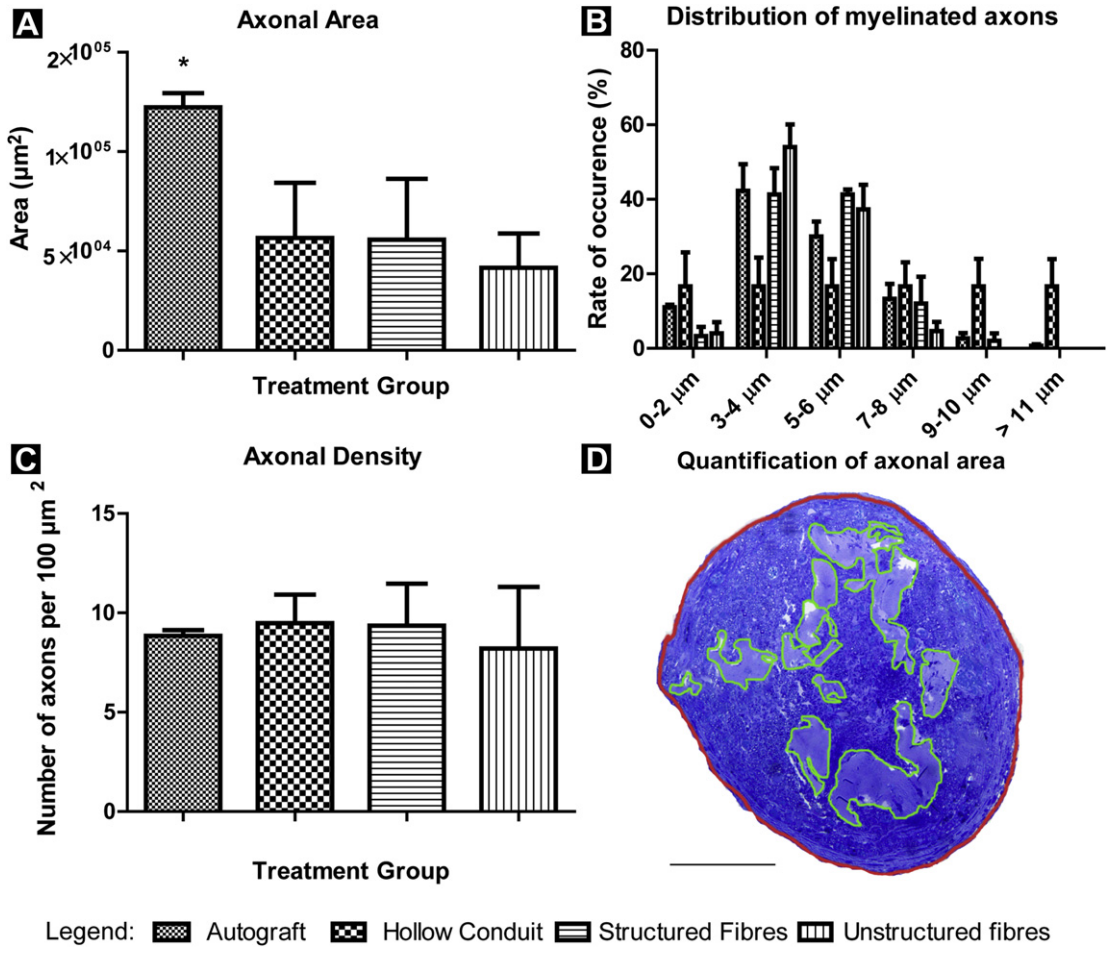

Fig. 6. Morphological analysis of axonal area, density and the axonal fibre distribution from the midgraft of the harvested neuronal tissue. (A) Autograft shows a significantly higher nerve regeneration area than all of the experimental conduit groups ($p < 0.05$). (B) Graph details the distribution of axons within the regenerated tissue across all experimental groups. Autograft and fibre groups show a higher proportion of myelinated axons with diameters in the range of 3–4 µm than that of control hollow conduits. (C) Graph shows no significant differences seen between all experimental group for axonal density. (D) Figure detailing procedure for quantification of axonal area. The axonal area was traced along its extremities (red) using image analysis software (ImageJ) and the overall axonal area (including the collagen fibres) was quantified. Collagen fibres present in the neural tissue was similarly traced (green) and the overall fibre area was quantified. The final axonal area used in (A) was calculated by subtracting the fibre area from the overall axonal area. (For interpretation of the references to colour in this figure legend, the reader is referred to the web version of this article.)

3.4. Histological & morphological analysis of implanted conduits

Tissue samples were explanted and prepared for tissue sectioning. Samples were embedded in spur resin and 1 µm thick sections were stained with 1% toluidine blue for visualisation under light microscopy. Images were taken initially at 100× magnification at the midpoint for general observations of nerve regeneration and for quantitative evaluation of nerve regeneration (Figs. 4 and 5).

3.4.1. Incorporation of intraluminal fibres into the host regenerative process

Initial qualitative analysis at 100× magnification, showed a nerve tissue cable to have grown within the outer conduit in all conduit groups (Fig. 4). For both fibre groups, the structured and unstructured fibres were seen to have been incorporated into the host regenerative process. The collagen fibres were intact and a number of axons were seen to be in close proximity to the fibres (Fig. 6 and 7). Similarly, a number of vascular bundles were seen throughout the tissue and in close approximation to the implanted fibres.

The total axonal area was quantified after subtracting the area occupied by the implanted collagen fibres (Fig. 5) at 100× magnification using ImageJ image analysis software. The autograft group showed a significantly greater axonal area versus all implanted conduit groups ($p < 0.05$) at midgraft region of the nerve. The nerve tissue area was quantified by subtracting the scaffold area from the overall area of nerve tissue.

Further quantification was carried out at 1000× magnification using a systematic stereological approach (Fig. 9). The number of myelinated fibres, axon density, mean myelinated fibre diameter, mean axonal fibre diameter, g-ratio and myelin thickness were evaluated and compared. Axonal density was seen to be similar across all conduit groups, with no statistical differences observed between groups ($p < 0.05$) (Fig. 5). Similarly, the autograft group displayed a significant higher number of regenerated axons at the midgraft level versus all experimental groups (10906.6 ± 195.11 axons). The scaffold area to nerve tissue area was similarly evaluated. No statistical differences were seen in terms of mean axonal and fibre diameters ($p < 0.05$). Myelin thickness and g-ratio were statistically improved for the autograft group versus all experimental groups ($p < 0.05$) (Fig. 8). The number of myelinated fibres was significantly greater in the autograft group versus the remaining experimental groups (10906.6 ± 195.11) ($p < 0.05$).

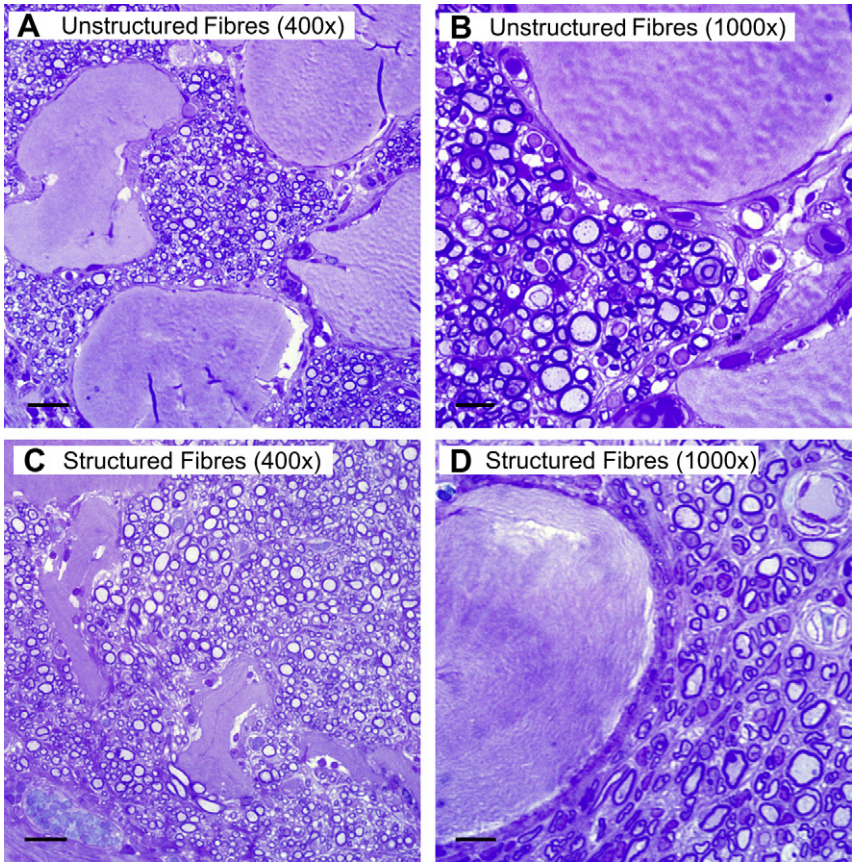

Fig. 7. Microscope images (toluidine blue stained) of unstructured (A and B) and structured (C and D) shown to have been successfully incorporated into the host regenerative process. Vascular cells can be seen to be growing in close proximity to the intraluminal fibres as well as a number of regenerated myelinated axons. Scale bars, 25 μm and 10 μm for 400× and 1000× images respectively.

4. Discussion

The use of intraluminal guidance structures is an important strategy for improving nerve regeneration in hollow nerve guidance conduits. These intraluminal fillers act as a replacement for or act as an anchor for the fibrin cable which forms during conduit mediated repair [18]. Strategies include the use of various types of scaffolds including gels, fibres, sponges and films. These fillers are made from a number of biological (collagen, fibrin, keratin) and artificial substrates (polylactic acid, poly(lactic-co-glycolic acid)) [6]. The addition of such intraluminal guidance structures or fillers results in changes in the response of regenerating axons and Schwann cells during repair. Localised effects occur on the growth cone of the regenerating axons in response to contact mediated intraluminal guidance cues. The effects of this localised signalling on nerve repair are still being realised [21]. These localised changes in signalling result in overall changes in the axonal regenerative response. In this investigation collagen fibres were used to assess their feasibility for nerve repair and to analyse the influence of these fibres on axonal dispersion within a hollow conduit. This study uses collagen as the major component for nerve repair. Collagen which comprises 30% of all proteins in the body is an essential component of nerve tissue [32]. Collagen is found in both the inner endoneurium (collagen type I and type II) and outer perineurium of peripheral nerves arranged in bundles of collagen fibres [33]. Collagen has a number of benefits for nerve repair. Advantages include controlled degradability (via crosslinking) and stability with minimal foreign body response which are very attractive properties for nerve repair.

Controlled crosslinking of the collagen allows degradation and tensile strength to be tailored for application in nerve repair. As can be seen the EDC:NHS cross-linked intraluminal collagen fibres were still visible within the lumen of the conduit up to 16 weeks after implantation (showing initial signs of degradation) and that axons were seen to have grown in close proximity to the implanted fibres (Fig. 6). Similarly the outer nerve guidance conduit, similarly made from collagen, was structurally intact after a period of 16 weeks with no instances of conduit collapse. Despite having not fully degraded, the intraluminal collagen fibres were shown not to significantly impede nerve regeneration. For nerve area calculations the scaffold area was subtracted from the total area to give a more representative quantification of nerve repair. It can be seen from the results that despite occupying space within the regenerated nerve cable there was no significant difference in nerve area between the fibre groups and the hollow nerve guidance conduit (Fig. 5) ($p < 0.05$). Instead regeneration occurred in close proximity to the fibres. For future studies higher levels of nerve regeneration may be achieved using collagen fibres which degrade quicker. The space which is currently still occupied by the intraluminal fibres could potentially be replaced by additional regenerating axons.

This study simultaneously investigates the incorporation of longitudinal micro-channels on the fibre surface. To date these micro-structured fibres have only been used in short term nerve regeneration studies (maximum of 6 weeks). This study characterises such a system in a long term nerve regeneration study (16 weeks) and compares them directly to their unstructured counterparts. The incorporation of additional topographical guidance features on the surface of the conduits was considered as

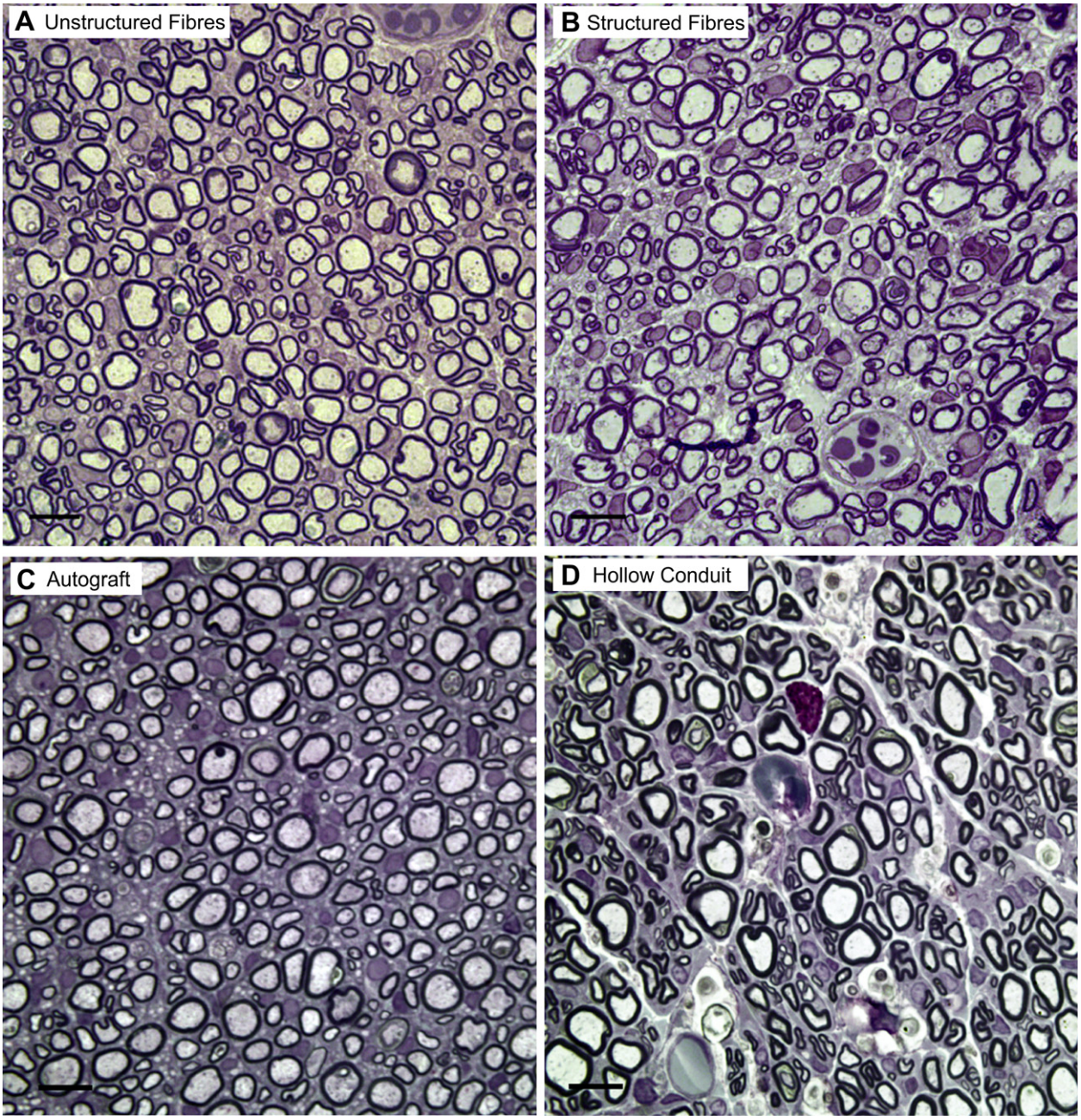

Fig. 8. Microscopic images (1000× magnification) of regenerated nerve at the midgraft level stained with 1% toluidine blue. Images shown represent the following groups: (A) unstructured fibres (B) structured fibres, (C) autograft and (D) hollow conduit. All scale bars, 10 μm.

a potential avenue to further improve nerve repair. It has been shown on flat PLGA films that micro-grooved surfaces as small as 5 μm and 10 μm in width increased aligned neurite outgrowth from PC12 cells [25].

Studies by Ribeiro et al. and later by Nichterwitz et al. have described the use of similar micro-structured intraluminal fibres both *in vitro* and *in vivo* [34,35]. In initial *in vitro* studies, micro-structured poly-ε-caprolactone (PCL) fibres displayed not only the ability both to support growth but also to facilitate increased alignment of Schwann cells and increased alignment of neurites extending from seeded rat dorsal root ganglion (DRG). The aligned Schwann cells also displayed increased L1 expression, known to be a marker for the switching of Schwann cells from a mature to a regenerative phenotype. These Schwann cells were said to form artificial glial Bands of Bungner, illustrating another benefit for repair. In a subsequent *in vivo* study, the PCL fibres were replaced with faster degrading poly-p-dioxanone (PDO) fibres and implanted in a rat sciatic nerve model using an epineurial sheath technique. Six weeks *post*-implantation; Schwann cells showed parallel and aligned migration along the fibres. Axons were seen to subsequently navigate through these Schwann cell bands. These studies further support the use of intraluminal fillers or their micro-structured counterparts.

Despite showing promising results, the aforementioned study had a number of limitations: the studies were carried out over a relatively short term (6 weeks versus 16 weeks in this current study), the study was carried out with no outer conduit, no comparisons of the micro-structured PDO fibres were made with

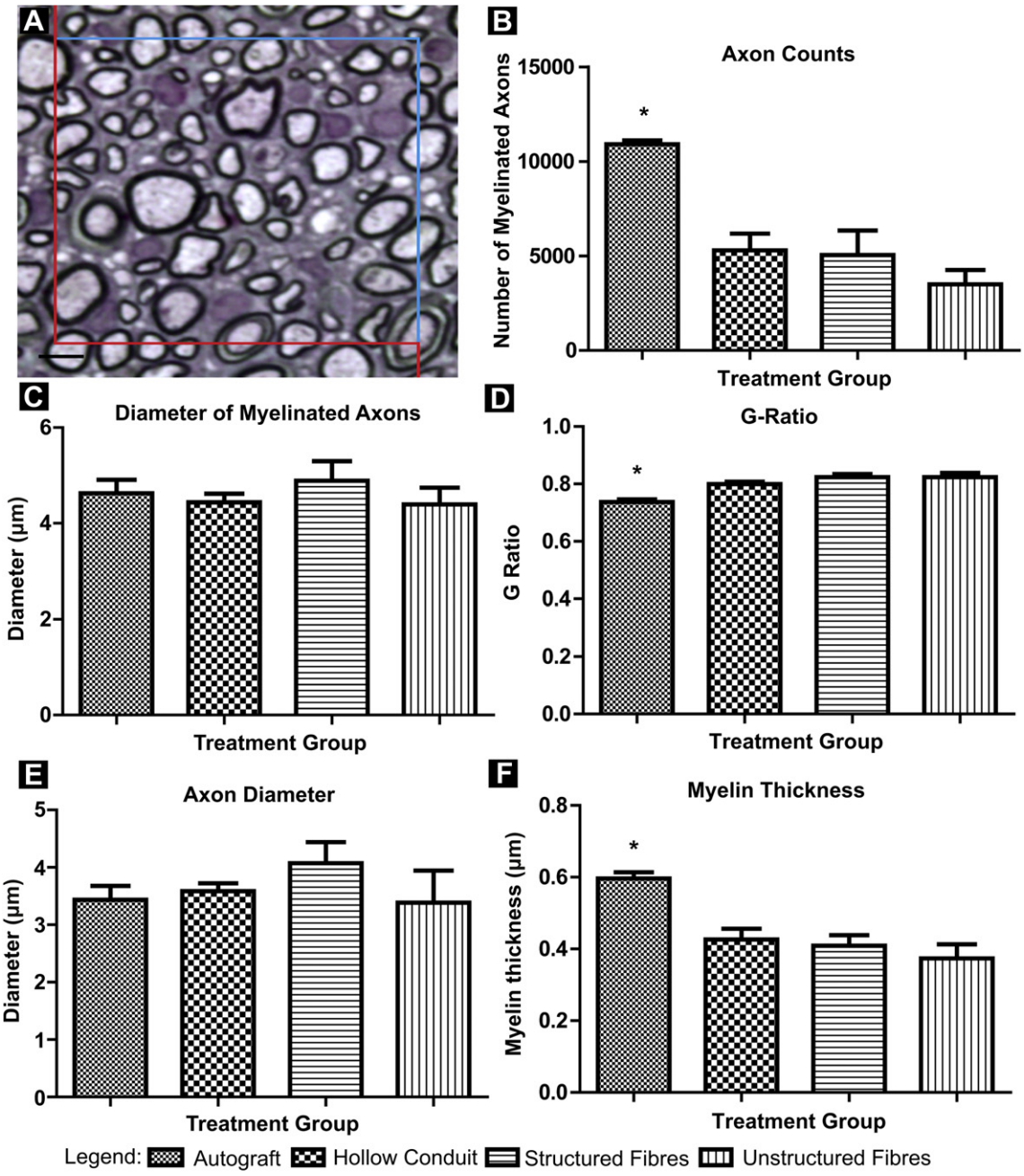

Fig. 9. Morphological analysis of regenerated nerve. (A) Diagram of stereological approach to quantify nerve regeneration. A 1600 μm^2 unbiased counting frame was applied to a nerve section which was selected in a systematic random manner from the overall nerve regeneration area. Inclusion lines are represented in blue (upper and right lines of the unbiased frame) and any axon profile interacting with these inclusion lines are included in the analysis. Exclusion lines are represented in red (lower and left lines of the unbiased frame) and any axon profiles interacting with these exclusion lines are not included in the analysis. Scale bar, 5 μm. (B) Axon counts show significantly more axonal profiles in the regenerated tissue of the autograft group versus all experimental groups ($p < 0.05$). (C) No significant difference was seen in the mean myelinated diameter between each experimental group ($p < 0.05$). (D) G-ratio was significantly lower in the autograft group versus all conduit groups. The ideal g-ratio is between 0.6 and 0.7 [30]. (E) There was no significant difference seen in the unmyelinated fibre diameter between all experimental groups ($p < 0.05$). (F) Autograft displayed a significant higher myelin thickness versus all the conduit groups ($p < 0.05$). (For interpretation of the references to colour in this figure legend, the reader is referred to the web version of this article.)

control groups (such as autograft and hollow conduit used here or similarly no comparisons between structured and unstructured fibres) and finally no quantification of nerve regeneration were made. Despite this, the proof of concept study elucidates benefits for the current investigation.

Herein, this study evaluates and compares such microstuctured fibres *in vivo* with their unstructured counterparts. Structuring of the fibres was carried out using an excimer laser system. The use of the excimer laser system allows precise control of a number of parameters (including groove width, groove depth and shape of the groove) when structuring the surface of the fibres (Table 2). Using the manufactured rotary stage in tandem with this system allowed the manufacture of collagen fibres with multiple longitudinal channels along their surface. Structuring of the surface however can become time-intensive especially if higher depths on the surfaces of the materials are required. For use as a tool outside these studies optimisation of each parameter would be required. The user needs to maintain a sufficient balance between time of production

and meeting the required structural requirements. For this study fibres with a diameter of approximately 50 μm were produced with a groove width of approximately 10 μm running longitudinally across its surface. The choice of this groove width was based on *in vitro* studies which demonstrated increased axonal alignment and growth, as well as guided Schwann cell migration and alignment [25]. Similar studies have shown that fibres of approximately 10–80 μm from a broad range of materials have been used successfully for peripheral nerve repair [13,36–40]. These fibres act as a platform for guided Schwann cell migration during the early stages of peripheral nerve repair while providing a means of topographical guidance to regenerating axons.

After 16 weeks implantation and despite the incorporation of additional structural guidance cues, there was a no significant difference present between the structured and unstructured fibre over a 16 week period ($p < 0.05$). There was a trend towards a slight increase in regeneration in the structured group versus their unstructured counterparts, although this trend was not deemed significant. The beneficial effect of such micro-structured fibres may be masked at such a late time point and may only have proven beneficial at the early stages of repair. Studies by Madduri et al. assessed the effect of aligned silk matrices versus their unaligned counterparts *in vitro*. This study showed that the introduction of an aligned matrix significantly increased Schwann cell migration and the rate of axonal growth after five days in culture [4]. Studies by Kim et al. and later by Clements et al. similarly allude to more efficient migration of Schwann cells and axonal regeneration through the addition of topographical guidance cues [18,21,41]. Similarly the introduction of structured fibres may have increased rates of migration and growth during the initial stages of repair.

However; addition of intraluminal fibres (either structured or unstructured) had distinct advantages for repair. In simultaneous retrograde tracing studies, intraluminal fibre groups displayed a significant reduction in axonal dispersion versus the autograft group ($p < 0.05$). Hence intraluminal fillers in this study were shown to consequently reduce axonal misdirection. Additionally the number of axons which were shown to be growing down their respective branches was statistically increased in comparison to using a hollow conduit alone. Ultimately, this response is likely to result in more defined muscle control for the end patient in the clinic. A further benefit for repair using either of the intraluminal fibre groups, was that the number of axons reaching their distal targets in both fibre groups was significantly greater than that of the hollow conduit group ($p < 0.05$). The combined results from retrograde tracing studies suggest a distinct advantage for repair through the use of intraluminal collagen fibres. Of note the use of autograft for peripheral nerve repair showed the highest amount of nerve regeneration. However, the rate of misdirection using autograft repair was significantly higher than the conduit groups. This high percentage of misdirected axons in autograft repair highlights another limitation of this treatment regime and the requirement for an alternative therapy. Ideally the replacement should match nerve regeneration levels seen in autograft while maintaining levels of axonal dispersion to a minimum.

To this end, intraluminal fibres have shown the ability to act as a supportive platform for growth and repair. They have shown the ability to guide axonal regeneration and to significantly reduce the levels of axonal mismatch during repair. The true benefits of such a system may only be realised over a critical nerve gap study (>15 mm in a rat). Future studies will aim towards targeting such a system. Despite showing distinct benefits for regeneration, levels of nerve regeneration remain lower than those of autograft. Future studies will focus on the creation of a more supportive environment for repair. This may be achieved through the addition of number of extrinsic factors [42]. These may be cellular (Schwann cells, stem cells) or molecular (neurotrophic factors, growth factors, ECM molecules) in nature and could aid in increasing overall levels of nerve regeneration.

5. Conclusions

Intraluminal collagen fibres provide beneficial effects for use in conduit mediated microsurgical repair of peripheral nerve injuries. Both structured and unstructured fibres become fully incorporated into the regenerative process and significantly reduce the level of axonal dispersion.

Acknowledgements

This material is based upon works supported by the Science Foundation Ireland under Grant No. 07/SRC/B1163 and Enterprise Ireland, Proof of Concept (PC/2008/399), co–funded by the European Regional Development Fund and Ireland's EU Structural Funds Programmes 2007–2013.

The author would also like to thank Mr. Anthony Sloan for all his help and support in the technical writing and preparation of the submitted manuscript. Prof. Peter Dockery for all his advice on stereology and the interpretation of microscopic images.

References

[1] Mukhatyar V, Karumbaiah L, Yeh J, Bellamkonda R. Tissue engineering strategies designed to realize the endogenous regenerative potential of peripheral nerves. Adv Mater 2009;21:4670–9.
[2] Siemionow M, Brzezicki G. Chapter 8: current techniques and concepts in peripheral nerve repair. In: Stefano G, Pierluigi T, Bruno B, editors. Int rev neurobiol. Academic Press; 2009. p. 141–72.
[3] Jiang X, Lim SH, Mao H-Q, Chew SY. Current applications and future perspectives of artificial nerve conduits. Exp Neurol 2010;223:86–101.
[4] Madduri S, Papaloïzos M, Gander B. Trophically and topographically functionalized silk fibroin nerve conduits for guided peripheral nerve regeneration. Biomaterials 2010;31:2323–34.
[5] Siemionow M, Bozkurt M, Zor F. Regeneration and repair of peripheral nerves with different biomaterials: review. Microsurgery 2010;30:574–88.
[6] Daly W, Yao L, Zeugolis D, Windebank A, Pandit A. A biomaterials approach to peripheral nerve regeneration: bridging the peripheral nerve gap and enhancing functional recovery. J R Soc Interface 2012;9:202–21.
[7] Pabari A, Yang SY, Seifalian AM, Mosahebi A. Modern surgical management of peripheral nerve gap. J Plast Reconstr Aesthet Surg 2010;63:1941–8.
[8] Belkas SJ, Shoichet SM, Midha Rajiv. Peripheral nerve regeneration through guidance tubes. Neurol Res 2004;26:10.
[9] Alluin O, Wittmann C, Marqueste T, Chabas J-F, Garcia S, Lavaut M-N, et al. Functional recovery after peripheral nerve injury and implantation of a collagen guide. Biomaterials 2009;30:363–73.
[10] Fu S, Gordon T. The cellular and molecular basis of peripheral nerve regeneration. Mol Neurobiol 1997;14:67–116.
[11] di Summa PG, Kalbermatten DF, Pralong E, Raffoul W, Kingham PJ, Terenghi G. Long-term in vivo regeneration of peripheral nerves through bioengineered nerve grafts. Neuroscience 2011;181:278–91.
[12] Toba T, Nakamura T, Shimizu Y, Matsumoto K, Ohnishi K, Fukuda S, et al. Regeneration of canine peroneal nerve with the use of a polyglycolic acid–collagen tube filled with laminin-soaked collagen sponge: a comparative study of collagen sponge and collagen fibers as filling materials for nerve conduits. J Biomed Mater Res 2001;58:622–30.
[13] Bozkurt A, Lassner F, O'Dey D, Deumens R, Böcker A, Schwendt T, et al. The role of microstructured and interconnected pore channels in a collagen-based nerve guide on axonal regeneration in peripheral nerves. Biomaterials 2012;33:1363–75.
[14] Lundborg G. A 25-year perspective of peripheral nerve surgery: evolving neuroscientific concepts and clinical significance. J Hand Surg Am 2000;25:391–414.
[15] Williams LR, Longo FM, Powell HC, Lundborg G, Varon S. Spatial-temporal progress of peripheral nerve regeneration within a silicone chamber: parameters for a bioassay. J Comp Neurol 1983;218:460–70.
[16] Koh HS, Yong T, Teo WE, Chan CK, Puhaindran ME, Tan TC, et al. In vivo study of novel nanofibrous intra-luminal guidance channels to promote nerve regeneration. J Neural Eng 2010;7:046003.
[17] Kim H, Tator CH, Shoichet MS. Design of protein-releasing chitosan channels. Biotechnol Prog 2008;24:932–7.
[18] Clements IP, Kim Y-t, English AW, Lu X, Chung A, Bellamkonda RV. Thin-film enhanced nerve guidance channels for peripheral nerve repair. Biomaterials 2009;30:3834–46.

[19] Lee D-Y, Choi B-H, Park J-H, Zhu S-J, Kim B-Y, Huh J-Y, et al. Nerve regeneration with the use of a poly(l-lactide-co-glycolic acid)-coated collagen tube filled with collagen gel. J Craniomaxillofac Surg 2006;34:50–6.
[20] Sierpinski P, Garrett J, Ma J, Apel P, Klorig D, Smith T, et al. The use of keratin biomaterials derived from human hair for the promotion of rapid regeneration of peripheral nerves. Biomaterials 2008;29:118–28.
[21] Hoffman-Kim D, Mitchel JA, Bellamkonda RV. Topography, cell response, and nerve regeneration. Annu Rev Biomed Eng 2010;12:203–31.
[22] Bozkurt A, Brook GA, Moellers S, Lassner F, Sellhaus B, Weis J, et al. In vitro assessment of axonal growth using dorsal root ganglia explants in a novel three-dimensional collagen matrix. Tissue Eng 2007;13:2971–9.
[23] Bozkurt A, Deumens R, Beckmann C, Olde Damink L, Schugner F, Heschel I, et al. In vitro cell alignment obtained with a Schwann cell enriched microstructured nerve guide with longitudinal guidance channels. Biomaterials 2009;30:169–79.
[24] Mahoney MJ, Chen RR, Tan J, Mark Saltzman W. The influence of microchannels on neurite growth and architecture. Biomaterials 2005;26:771–8.
[25] Yao L, Wang S, Cui W, Sherlock R, Oconnell C, Damodaran G, et al. Effect of functionalized micropatterned PLGA on guided neurite growth. Acta Biomater 2009;5:580–8.
[26] Zeugolis DI, Paul RG, Attenburrow G. Post-self-assembly experimentation on extruded collagen fibres for tissue engineering applications. Acta Biomater 2008;4:1646–56.
[27] Zeugolis DI, Paul GR, Attenburrow G. Cross-linking of extruded collagen fibers—a biomimetic three-dimensional scaffold for tissue engineering applications. J Biomed Mater Res A 2009;89A:895–908.
[28] Fantes FE, Waring GO. Effect of excimer laser radiant exposure on uniformity of ablated corneal surface. Lasers Surg Med 1989;9:533–42.
[29] McDowell EM, Trump BF. Histologic fixatives suitable for diagnostic light and electron microscopy. Arch Pathol Lab Med 1976;100:405–14.
[30] Stang F, Fansa H, Wolf G, Reppin M, Keilhoff G. Structural parameters of collagen nerve grafts influence peripheral nerve regeneration. Biomaterials 2005;26:3083–91.
[31] Canan S, Bozkurt HH, Acar M, Vlamings R, Aktas A, Sahin B, et al. An efficient stereological sampling approach for quantitative assessment of nerve regeneration. Neuropathol Appl Neurobiol 2008;34:638–49.
[32] Wolfgang F. Collagen – biomaterial for drug delivery. Eur J Pharm Biopharm 1998;45:113–36.
[33] Kaplan S, Odaci E, Unal B, Sahin B, Fornaro M. Chapter 2: development of the peripheral nerve. In: Stefano G, Pierluigi T, Bruno B, editors. Int rev neurobiol. Academic Press; 2009. p. 9–26.
[34] Ribeiro-Resende VT, Koenig B, Nichterwitz S, Oberhoffner S, Schlosshauer B. Strategies for inducing the formation of bands of Büngner in peripheral nerve regeneration. Biomaterials 2009;30:5251–9.
[35] Nichterwitz S, Hoffmann N, Hajosch R, Oberhoffner S, Schlosshauer B. Bioengineered glial strands for nerve regeneration. Neurosci Lett 2010;484:118–22.
[36] Yang Y, Ding F, Wu J, Hu W, Liu W, Liu J, et al. Development and evaluation of silk fibroin-based nerve grafts used for peripheral nerve regeneration. Biomaterials 2007;28:5526–35.
[37] Ngo T-TB, Waggoner PJ, Romero AA, Nelson KD, Eberhart RC, Smith GM. Poly(L-lactide) microfilaments enhance peripheral nerve regeneration across extended nerve lesions. J Neurosci Res 2003;72:227–38.
[38] Cai J, Peng X, Nelson KD, Eberhart R, Smith GM. Permeable guidance channels containing microfilament scaffolds enhance axon growth and maturation. J Biomed Mater Res A 2005;75A:374–86.
[39] Yoshii S, Oka M, Shima M, Taniguchi A, Akagi M. Bridging a 30-mm nerve defect using collagen filaments. J Biomed Mater Res A 2003;67A:467–74.
[40] Matsumoto K, Ohnishi K, Kiyotani T, Sekine T, Ueda H, Nakamura T, et al. Peripheral nerve regeneration across an 80-mm gap bridged by a polyglycolic acid (PGA)-collagen tube filled with laminin-coated collagen fibers: a histological and electrophysiological evaluation of regenerated nerves. Brain Res 2000;868:315–28.
[41] Kim YT, Haftel VK, Kumar S, Bellamkonda RV. The role of aligned polymer fiber-based constructs in the bridging of long peripheral nerve gaps. Biomaterials 2008;29:3117–27.
[42] Nectow AR, Marra KG, Kaplan DL. Biomaterials for the development of peripheral nerve guidance conduits. Tissue Eng Part B, Rev 2012;18:40–50.